J. Fluid Mech. (1995), *vol.* 297, *pp.* 255–273

Standing and travelling oscillatory blob convection

By R. M. CLEVER AND F. H. BUSSE

Institute of Geophysics and Planetary Physics, UCLA, Los Angeles, CA 90024, USA
and Institute of Physics, University of Bayreuth, D-95440 Bayreuth, Germany

(Received 18 July 1994 and in revised form 21 April 1995)

Results of numerical computations are presented of time-dependent three-dimensional convection flows in a horizontal layer heated from below which evolve from the oscillatory blob instability of steady two-dimensional rolls. It is shown that the heat transport is typically increased in the transition to blob convection. Oscillatory blob convection exists in the forms of standing or travelling blob convection. The latter type of solution represents the stable form bifurcating supercritically at the Rayleigh number R_{II} for the onset of the oscillatory blob instability. In contrast to standing blob convection travelling blob convection exhibits a mean flow.

1. Introduction

Rayleigh–Bénard convection in a layer heated from below has become one of the principal examples in fluid dynamics of the evolution from simple to complex flows with increasing control parameter. When the properties of the layer are symmetric about the midplane, flows in the form of two-dimensional rolls are found as stable steady solutions for perfectly conducting rigid boundaries. We shall call these rolls secondary solutions of the problem since they replace the basic state of the layer when the Rayleigh number R exceeds its critical value. As the control parameter R is increased further, a number of different transitions is encountered depending on the Prandtl number of the fluid. The instabilities causing these transitions have been investigated in a number of papers starting with the early work of Busse (1967) up to the latest papers on the subject by Bolton, Busse & Clever (1986) and by Clever & Busse (1990). For reviews we refer to Busse (1981) and to Busse & Clever (1990). The analysis of the tertiary forms of convection evolving from these instabilities has not yet been completed. Steady bimodal convection in high Prandtl number fluids has been investigated by Frick, Busse & Clever (1983) and travelling wave convection realized in low Prandtl number fluids is described by Clever & Busse (1987, 1989, 1990). At intermediate Prandtl numbers steady knot convection represents another stable tertiary state of the system (Clever & Busse 1988). Finally, in this paper results for oscillatory blob convection will be presented which competes with knot convection in the parameter space of the problem. Tertiary states induced by the skewed varicose instability (Busse & Clever 1979) do not seem to lead to states that are steady or time periodic. Instead, experimental observations (Gollub, McCarriar & Steinman 1982) and numerical simulations (Zippelius & Siggia 1983) tend to suggest a transition into an irregular state of convection which is aperiodic in space and time. For a recent study of the evolution of skewed varicose disturbances in the presence of stress-free boundaries we refer to Busse, Kropp & Zaks (1992).

While some properties of the thermal blob instability have already been discussed by Bolton *et al.* (1986) the finite-amplitude properties of this type of oscillatory convection are of interest for several reasons. Nearly periodic eruptions of thermal blobs from boundary layers have often been observed in experiments and have been described in Howard's (1966) boundary-layer model of turbulent convection. The thermal blobs represent a main feature in high Rayleigh number convection as shown in modern experiments by Zocchi, Moses & Libchaber (1990) and Solomon & Gollub (1990). The basic mechanism of this time-dependent form of convection can be described in a quantitative way most easily in the form of oscillatory blob convection. Since thermal blob convection occurs primarily in the form of a wave travelling along the basic convection roll, a preferred direction is introduced. A mean flow associated with the wave becomes possible as will be shown in this paper. This effect may explain some puzzling experimental observations since all other instabilities of convection rolls do not seem to lead to a generation of mean flows in fluids with Prandtl numbers of the order two or larger. Oscillatory thermal blob convection has also been found in numerous numerical simulations, for instance in those of Curry *et al.* (1984) for the case of stress-free boundaries or in the work of Lennie *et al.* (1988) on infinite Prandtl number convection. In the present paper a more systematic approach to the problem is used and the phenomenon of travelling blob convection is described for the first time.

Because the numerical methods employed in the present analysis are the same as those employed in previous work (Clever & Busse, 1987, 1988), only a brief outline of the mathematical formulation of the problem and of the numerical procedures is given in §2.

2. Mathematical description of the problem

We consider a horizontal fluid layer of height h with rigid upper and lower boundaries that are kept at the constant temperatures T_1 and T_2, respectively. Using h as length scale, h^2/κ as time scale, where κ is the thermal diffusivity, and $(T_2-T_1)/R$ as temperature scale we can write the basic equations in their usual (see, for instance, Busse 1981) dimensionless form,

$$\left(\frac{\partial}{\partial t}\boldsymbol{v}+\boldsymbol{v}\cdot\nabla\boldsymbol{v}\right)P^{-1}=-\nabla\pi+\boldsymbol{k}\theta+\nabla^2\boldsymbol{v}, \tag{2.1a}$$

$$\nabla\cdot\boldsymbol{v}=0, \tag{2.1b}$$

$$\left(\frac{\partial}{\partial t}+\boldsymbol{v}\cdot\nabla\right)\theta=\boldsymbol{k}\cdot\boldsymbol{v}+\nabla^2\theta. \tag{2.1c}$$

The Boussinesq approximation has been assumed in which the variation of density is neglected except in the gravity term where a linear dependence of the density on temperature is taken into account. θ denotes the deviation of the temperature from the static distribution. Since the velocity field $\boldsymbol{v}$ is solenoidal, we can use the following general representation:

$$\boldsymbol{v}=\nabla\times(\nabla\times\boldsymbol{k}\varphi)+\nabla\times\boldsymbol{k}\psi+U\boldsymbol{i}$$

where $\boldsymbol{k}$ is the vertical unit vector parallel to the z-axis of the Cartesian system of coordinates that we shall use and $U(z)$ describes a mean flow in the direction of the horizontal unit vector $\boldsymbol{i}$. The mean flow could be presented through the stream function ψ. But in that case ψ would no longer be a bounded function (Schmitt &

von Wahl 1992). By taking the z-components of the (curl)^2 and of the curl of the equation of motion we obtain the following equations for φ and ψ:

$$\nabla^4\Delta_2\varphi - \Delta_2\theta = P^{-1}\{\boldsymbol{k}\cdot\nabla\times[\nabla\times(\boldsymbol{v}\cdot\nabla\boldsymbol{v})] + \frac{\partial}{\partial t}\nabla^2\Delta_2\varphi\}, \tag{2.2a}$$

$$\nabla^2\Delta_2\psi = P^{-1}\{-\boldsymbol{k}\cdot\nabla\times[\boldsymbol{v}\cdot\nabla\boldsymbol{v}] + \frac{\partial}{\partial t}\Delta_2\psi\} \tag{2.2b}$$

where Δ_2 denotes the horizontal Laplacian, $\Delta_2 \equiv \partial^2/\partial x^2 + \partial^2/\partial y^2$. The heat equation (2.1$c$) can be rewritten in the form

$$\nabla^2\theta - R\Delta_2\varphi = (\nabla\times(\nabla\times\boldsymbol{k}\varphi) + \nabla\times\boldsymbol{k}\psi + U\boldsymbol{i})\cdot\nabla\theta + \frac{\partial}{\partial t}\theta \tag{2.2c}$$

The Rayleigh number R and the Prandtl number P are defined by

$$R = \frac{\gamma g(T_2 - T_1)h^3}{\nu\kappa}, \quad P = \frac{\nu}{\kappa}$$

where γ is the thermal expansivity, g denotes the acceleration of gravity and ν is the kinematic viscosity. The mean flow U obeys the equation

$$\left(\frac{\partial^2}{\partial z^2} - P^{-1}\frac{\partial}{\partial t}\right)U = -\frac{\partial}{\partial z}\overline{(\Delta_2\varphi(\partial_{xz}^2\varphi + \partial_y\psi))}P^{-1} \tag{2.2d}$$

where the bar indicates the average over the (x, y)-plane. The boundary conditions are given by

$$\varphi = \frac{\partial}{\partial z}\varphi = \psi = \theta = U = 0 \quad \text{at} \quad z = \pm\tfrac{1}{2}. \tag{2.3}$$

As in previous work on three-dimensional convection (Clever & Busse, 1987, 1988) we use the Galerkin method for solving equations (2.2) together with conditions (2.3). We thus expand all dependent variables into a complete set of functions satisfying the boundary conditions

$$\varphi = \sum_{l,m,n}\{\hat{a}_{lmn}(t)\cos l\alpha_x(x-ct) + \check{a}_{lmn}(t)\sin l\alpha_x(x-ct)\}\cos(m\alpha_y y)g_n(z), \tag{2.4a}$$

$$\theta = \sum_{l,m,n}\{\hat{b}_{lmn}(t)\cos l\alpha_x(x-ct) + \check{b}_{lmn}(t)\sin l\alpha_x(x-ct)\}\cos(m\alpha_y y)\sin n\pi(z+\tfrac{1}{2}), \tag{2.4b}$$

$$\psi = \sum_{l,m,n}\{\hat{c}_{lmn}(t)\sin l\alpha_x(x-ct) + \check{c}_{lmn}(t)\cos l\alpha_x(x-ct)\}\sin(m\alpha_y y)\sin n\pi(z+\tfrac{1}{2}), \tag{2.4c}$$

$$U = \sum_n U_n(t)\sin n\pi(z+\tfrac{1}{2}), \tag{2.4d}$$

where $g_n(z)$ are the Chandrasekhar functions defined by

$$g_n(z) = \begin{cases} \sinh(\beta_{\frac{1}{2}n}z)(\sinh\tfrac{1}{2}\beta_{\frac{1}{2}n})^{-1} - \sin(\beta_{\frac{1}{2}n}z)(\sin\tfrac{1}{2}\beta_{\frac{1}{2}n})^{-1} & \text{for even } n \\ \cosh(\gamma_{\frac{1}{2}(n+1)}z)(\cosh\tfrac{1}{2}\gamma_{\frac{1}{2}(n+1)})^{-1} - \cos(\gamma_{\frac{1}{2}(n+1)}z)(\cos\tfrac{1}{2}\gamma_{\frac{1}{2}(n+1)})^{-1} & \text{for odd } n \end{cases}$$

and where the values β_ν and γ_ν are determined as positive roots of the equations

$$\coth\tfrac{1}{2}\beta - \cot\tfrac{1}{2}\beta = 0\ , \quad \tanh\tfrac{1}{2}\gamma + \tan\tfrac{1}{2}\gamma = 0$$

such that $g_n = g_n' = 0$ holds at $z = \pm 0.5$.

The time-dependence appears twice in each term of the presentation (2.4), but one of these dependences will be dropped in both cases of the following analysis. In the case

of standing oscillations the phase velocity c vanishes, while in the case of travelling waves all coefficients $\hat{a}_{lmn}, \check{a}_{lmn}, \hat{b}_{lmn}$ etc. can be regarded as time independent, since the entire time dependence of the travelling waves vanishes in the reference frame moving with c in the x-direction.

In writing expressions (2.4) we have used the property that the disturbances leading to the oscillatory blob instabilities (Bolton *et al.* 1986) preserve the vertical symmetry planes, $y = m\pi/\alpha_y$ for $m = 0, \pm 1, \ldots$, of the two-dimensional steady convection rolls. From this symmetry it also follows that a mean flow can only be directed in the x-direction as we have anticipated in formulating the representations (2.1), (2.4).

After multiplying equations (2.2) by the corresponding expansion functions of expressions (2.4) and averaging the result over the fluid layer, we obtain a system of ordinary differential equations in time for the coefficients $\hat{a}_{lmn}, \check{a}_{lmn}, \hat{b}_{lmn} \ldots$. This system can be integrated in time numerically after a truncation has been introduced. We shall neglect all coefficients and corresponding equations that satisfy

$$l + m + n > N_T \ . \tag{2.5}$$

By comparing solutions obtained for N_T with those for which $N_T - 2$ was used, we can check the quality of the numerical approximation. Typically N_T was chosen such that the Nusselt number changed by less than 1% in this comparison. For the numerical integration in time the Crank–Nicolson method was used. In some cases the Adams–Bashforth method was used for the purpose of comparisons. Provided the time step was chosen sufficiently small, typically $\Delta t = 10^{-3}$, the results obtained from both methods agree very well. In the case of the travelling blob convection time-independent coefficients $\hat{a}_{lmn}$ etc. can be assumed, but the finite phase velocity c must be determined. Because a shift in time $t' = t + t_0$ corresponds to a change in the coefficients $\hat{a}_{lmn}, \check{a}_{lmn}$, etc.,

$$\hat{a}'_{lmn} = \hat{a}_{lmn} \cos ct_0 - \check{a}_{lmn} \sin ct_0,$$
$$\check{a}'_{lmn} = \hat{a}_{lmn} \sin ct_0 + \check{a}_{lmn} \cos ct_0,$$

we can choose t_0 such that one coefficient, say $\check{a}_{112}$ vanishes. By using this freedom of choice for the phase we obtain the equation corresponding to the coefficient $\check{a}_{112}$ as an equation for c. The system of nonlinear algebraic equations can then be solved by a Newton–Raphson method in the same way as in the case of steady convection flows.

The fact that travelling blob convection is equivalent to steady convection in the moving frame of reference permits a straightforward application of the usual stability analysis of steady convection. By imposing infinitesimal disturbances of the form

$$\tilde{\phi} = \sum_{l,m,n} \tilde{a}_{lmn} \exp\{\mathrm{i}(l\alpha_x + d)(x - ct) + \mathrm{i}(m\alpha_y + b)y + \sigma t\} g_n(z), \tag{2.6a}$$

$$\tilde{\theta} = \sum_{l,m,n} \tilde{b}_{lmn} \exp\{\mathrm{i}(l\alpha_x + d)(x - ct) + \mathrm{i}(m\alpha_y + b)y + \sigma t\} \sin n\pi(z + \tfrac{1}{2}), \tag{2.6b}$$

$$\tilde{\psi} = \sum_{l,m,n} \tilde{c}_{lmn} \exp\{\mathrm{i}(l\alpha_x + d)(x - ct) + \mathrm{i}(m\alpha_y + b)y + \sigma t\} \sin n\pi(z + \tfrac{1}{2}) \tag{2.6c}$$

onto the travelling blob solutions of the form (2.4) with constant coefficients $\hat{a}_{lmn}, \ldots$ we obtain a linear homogeneous system of equations for the coefficients $\tilde{a}_{lmn}, \tilde{b}_{lmn}, \tilde{c}_{lmn}$ with the growth rate σ as the eigenvalue. For a given travelling blob solution characterized by the parameters $R, P, c, \alpha_x, \alpha_y$ the maximum real part σ_r of σ must be

determined as a function of the Floquet parameters d and b. When a positive σ_r exists, the travelling blob solution is unstable; otherwise it is regarded as stable. Owing to the complex notation used in expressions (2.6) the subscripts l, m run through positive as well as negative integer values and the truncation condition (2.5) thus has to be applied for $| l |$ and $| m |$ instead of l and m. Accordingly the system of disturbance equations becomes approximately four times as large as the system for the stationary travelling blob solution. Fortunately, for many instabilities σ_r reaches its maximum for $b = d = 0$ in which case considerable simplifications of the stability analysis become possible based on the symmetries of the travelilng blob solution. These simplifications will be discussed in §5.

3. Travelling blob convection

The time-dependent three-dimensional convection flows considered in this paper arise from the BO2-type oscillatory blob instability of convection rolls that was found by Bolton *et al.* (1986). Two blobs of fluid that are slightly hotter and two blobs that are slightly colder than the average temperature at their instantaneous position travel around the convection rolls. In addition the phase of this oscillation varies with the wavenumber α_x along the axis of the rolls. Because we are focusing on oscillations with two blobs we can use the symmetry that all coefficients $\hat{a}_{lmn}, \check{a}_{lmn}, \hat{b}_{lmn}, \check{b}_{lmn}, \hat{c}_{lmn}, \check{c}_{lmn}$ vanish unless

$$l + m + n = \text{ even integer.} \tag{3.1}$$

This includes, of course, for $l = 0$ the basic symmetry of the convection rolls. Because of the translation and reflection symmetries of the convection rolls along their axis, the oscillatory instability can lead to either travelling waves propagating in the positive or the negative x-direction along the rolls or it can lead to a standing oscillation. We first consider the travelling type of oscillatory blob convection. In choosing the values of the parameters R, P, α_x, α_y we are guided by the results of Bolton *et al.* (1986) who have computed the growth rates of the strongest growing blob instabilities as a function of α_x for given steady roll solutions characterized by fixed values of R, P and α_y. The results show that the BO2-instability corresponding to two circulating blobs occurs in the regime $2 \leqslant P \leqslant 10$ for values of α_y of the order 2 or lower. Since the growthrates exhibit a rather broad maximum as a function of α_x, we have selected a few values which we expect to be typical for eventual experimental realizations.

The geometrical configuration of the hot blobs circulating around the convection roll is sketched in figure 1. Intermediate between the two bands of hot blobs there are analogous bands of cold blobs that are not shown in the figure. The time dependence induced by the circulating blobs is shown in figure 2. The first plot of isotherms in the time sequence of seven plots exhibits rising and descending plumes that are colder than their time average while the thermal boundary layers near the feet of the plumes are warmer than their time average. We use the term 'plumes' we refer to the cross-section of the steady hot and cold sheets of fluids rising and descending, respectively, on either side of the convection roll. The plumes become colder than their time average because parcels or blobs of colder than average fluid travel along them strengthening the descending cold plume and weakening the ascending hot plume. As a consequence the strong cold plume accelerates the descending motion while the weak plume decelerates the ascending motion as is indicated in the corresponding streamline plot on the right half of the figure. As time progresses the situation reverses. The hot blobs from the boundary layer enter the respective plumes and

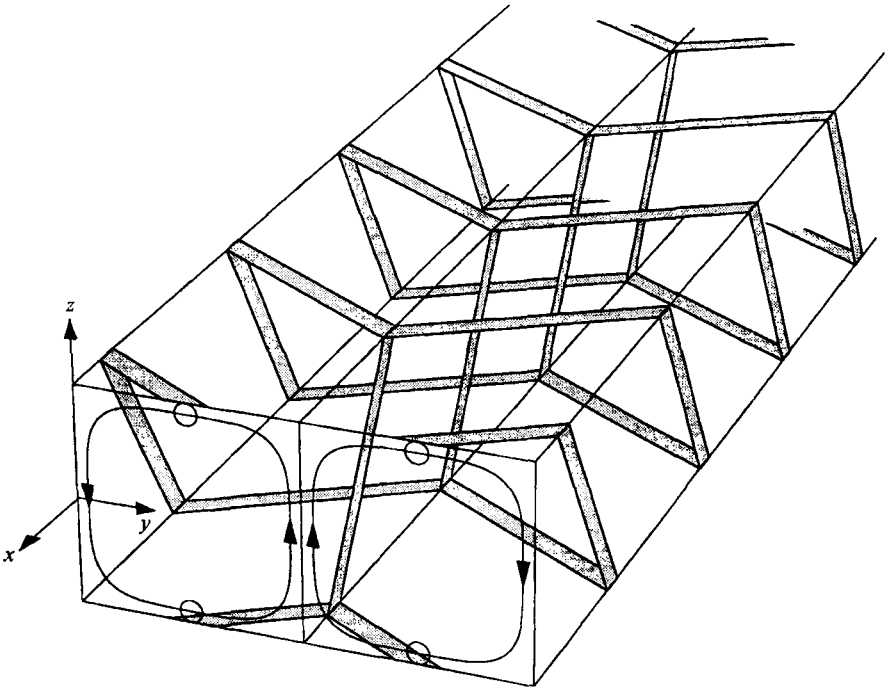

FIGURE 1. Sketch of travelling blob convection at a given instant in time. Regions where the fluid near the boundary of a roll is hotter than its time-averaged temperature are indicated by the bands on the roll boundary. The pattern propagates in the positive x-direction.

cause a strengthening of the hot and a weakening of the cold plume. The place where the streamlines come close together has now moved to the rising plume. The original cold blobs of the plumes have entered the thermal boundary layer causing a thinning of the bottom boundary layer and a thickening of the top boundary layer as is evident from the third and fourth plots of the sequence. In the remaining plots the situation reverses again until the seventh plot exhibits the same pattern as the first plot. Instead of interpreting the seven plots as a sequence in time at a given position in x we could also consider them, of course, as plots of the planes $x = n\pi/3\alpha_x, n = 0, 1, \ldots, 6$ at a given instant of time.

In order to provide a better impression of the three-dimensional nature of travelling blob convection we exhibit its pattern in figures 3 and 4 in planes orthogonal to the planes of figure 2. In figure 3 the pattern of travelling blob convection is shown through plots of the x,y-dependence of several variables. Since the pattern is steady with respect to the reference frame travelling with the speed $c = \omega/\alpha_x$ in the negative x-direction, the same process discussed in the case of figure 2 can be followed here by moving towards higher values of x. In particular the plots for the plane $z = -0.4$ show clearly the movements of hot blobs (rising motion) and cold blobs (descending motion) towards the rising plumes.

The strengthening and weakening of the hot and cold plumes can also be seen in the isotherms in the vertical planes $y = 0$ and $y = \pi/\alpha_y$, respectively, shown in figure 4. Because the pattern is moving steadily, the isotherms have been drawn for a single instant in time only. Since the pattern moves towards the left, the time dependence at a fixed position can be obtained by moving towards increasing x. For

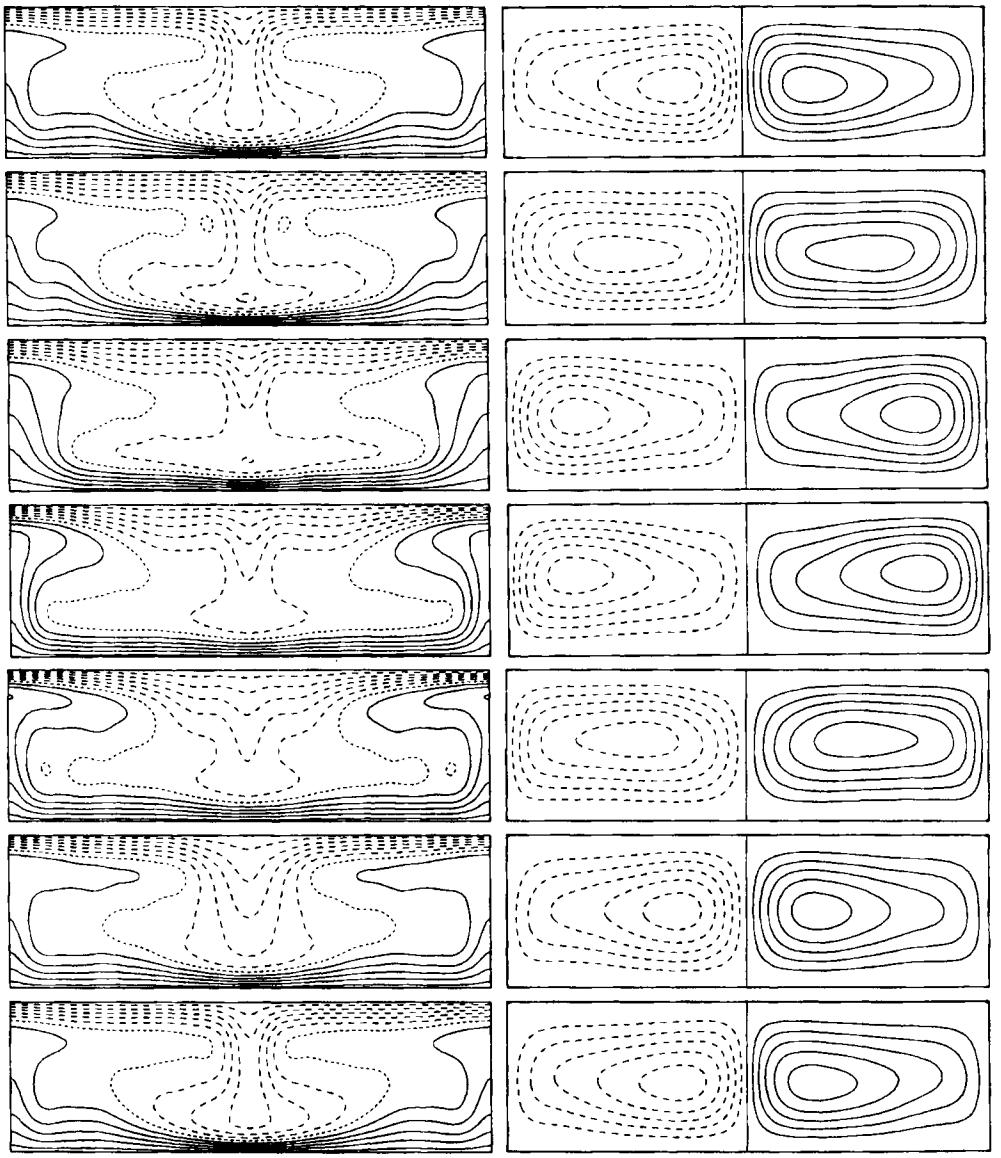

FIGURE 2. Isotherms (left) and streamlines $\partial\varphi/\partial y$ = const. (right) in the plane $x = 0$ of travelling blob convection with $R = 35000, P = 7, \alpha_x = \alpha_y = 2.0$. Time increases from top to bottom in steps of $\Delta t = 0.00567$ such that about a period, $T_p = 0.034$, has passed between the first and the last plot. The y-coordinate runs left to right from 0 to $2\pi/\alpha_y$ in each plot. Here and in the following figures all contour lines are plotted at equi-distant intervals with solid (dashed) lines denoting positive (negative) values. The dotted line indicates zero. Wherever a dotted line is not shown, the solid line adjacent to the dashed lines denotes zero.

completeness the isotherms are also shown for the vertical plane $y = \pi/2\alpha$ where only the thickening and thinning of the thermal boundary layers can be seen. Also shown in figure 4 are the lines of constant $\partial\varphi/\partial x$ which describe the part of motion that recirculates within the planes y =const. An important property of this motion is a finite Reynolds stress $\overline{v_z v_x}^x$ generated by the inclination of the rising and descending streamlines with respect to the vertical. As indicated by the superscript x this average

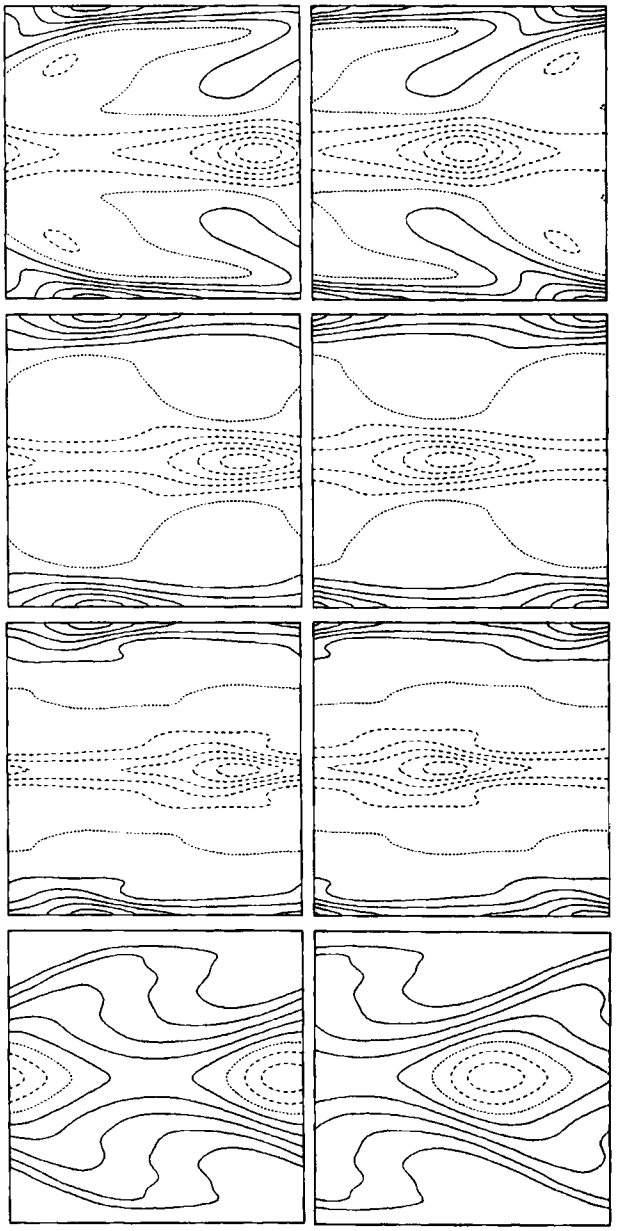

FIGURE 3. Lines of constant vertical velocity in the planes $z = -0.4$ (top row) and $z = 0$ (second row) and isotherms in the planes $z = 0$ (third row) and $z = -0.4$ (bottom row) are shown for travelling blob convection with the same parameters as in figure 2. The left plot corresponds to the same time as the second plot of figure 2, while the right plot corresponds to a time 0.01133 later.

is taken over lines of constant y and z. The Reynolds stress contributes to the non-vanishing x-average of the x-component of the velocity field which is shown in figure 5. As can be seen from the plots, a negative x-component dominates at $y = 0$ (left side of the plots) while a somewhat weaker positive x-velocity can be seen at $y = \pi/\alpha_y$ corresponding to the middle of the plots. Since the x-velocity v_x satisfies

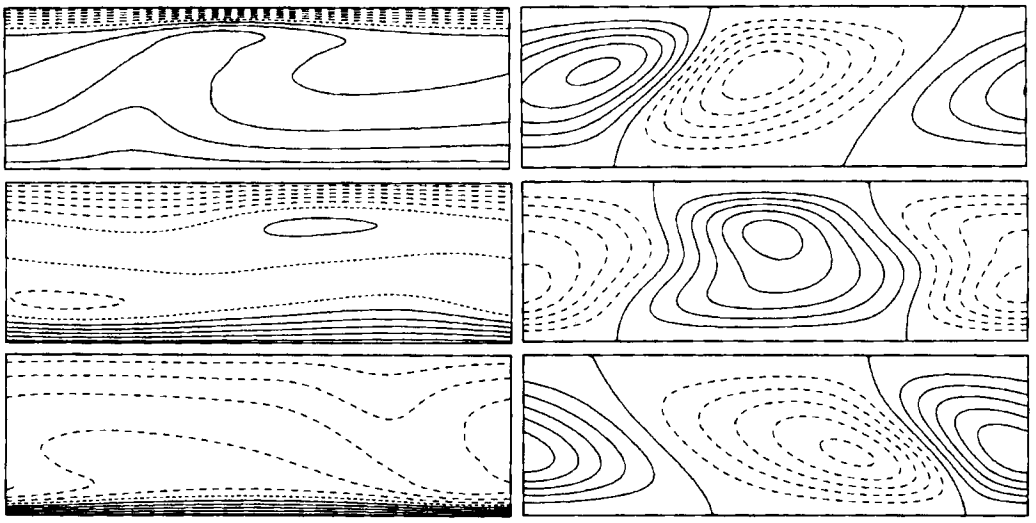

FIGURE 4. Isotherms (left) and streamlines $\partial\varphi/\partial x = \text{const.}$ (right) in the planes $y = 0, \pi/2\alpha_y, \pi/\alpha_y$ (from top to bottom) for travelling blob convection with same parameter values as for figure 2. The time corresponds to the left plots of figure 3 and x runs left to right from 0 to $2\pi/\alpha_x$ in each plot.

the symmetry relationship

$$v_x(x, y, z, t) = v_x(x + \pi/\alpha_x, -y + \pi/\alpha_y, -z, t) \tag{3.2}$$

a mean flow in the negative x-direction results. In other words, the 'mean' Reynolds stress defined by the horizontally averaged quantity $\overline{v_z v_x}$ is positive (negative) for most of the upper (lower) half of the layer in the case of a wave travelling in the negative x-direction. This phenomenon is caused by the fact that the rising plume tends to concentrate the flow towards the upper boundary, while the opposite is done by the descending plume. Figure 6 shows the mean flow created in this fashion along the axis of the rolls in the direction of the propagating wave.

While we have emphasized so far the circulation of blobs with the basic roll velocity, there is another aspect of the thermal blob mechanism which was first proposed by Howard (1966). Since heat transport of the rolls does not increase sufficiently with increasing Rayleigh number R to keep the thermal boundary layers stable in terms of the Rayleigh criterion for the stability of a fluid layer heated from below, periodic eruptions from the thickening thermal boundary layers must be expected. These eruptions may be identified with the ridges of vertical motion seen in the plane $z = -0.4$ of figure 3. Oscillatory blob convection may thus be regarded as a kind of resonance phenomenon between the periodic eruption from the thermal boundary layers and a simple fraction of the circulation period of the basic roll velocity as has been observed in a related context by Lennie *et al.* (1988). Similar relationships can be seen in other types of oscillatory convection with circulating thermal blobs as for example in oscillatory knot convection (Clever & Busse, 1989) or oscillatory bimodal convection (Clever & Busse, 1994). As in these latter cases, the thermal blobs contribute significantly to the convective heat transport as is evident from the comparison of the heat transports of two-dimensional rolls and of three-dimensional blob convection shown in figure 7.

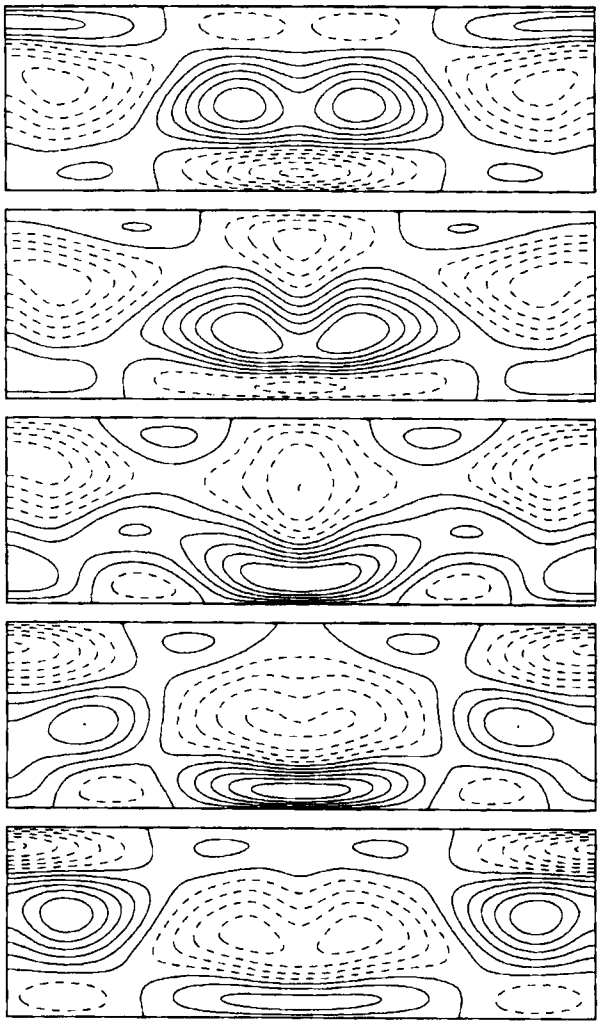

FIGURE 5. Lines of constant x-velocity, u_x, in the planes $x = n\pi/4\alpha_x$ for $n = 0,\ldots,4$ (from top to bottom) for travelling blob convection with $P = 2.5, R = 35000, \alpha_x = \alpha_y = 2.0$. Solid (dashed) lines indicate positive (negative) values except for the solid line adjacent to the dashed ones which indicates zero.

The oscillatory blob solutions bifurcating from the two-dimensional roll solutions are also characterized by a more efficient release of potential energy and a corresponding increase of the kinetic energy

$$E_{pol} = \tfrac{1}{2}\langle |\nabla \times (\nabla \times \boldsymbol{k}\varphi)|^2 \rangle \tag{3.3}$$

of the poloidal component of motion which parallels the increase of the Nusselt number as shown in figure 8. Because of the three-dimensional nature of oscillatory blob convection the toroidal component of the velocity described by the function ψ does not vanish as in the case of rolls. The kinetic energy

$$E_{tor} \equiv \tfrac{1}{2}\langle |\nabla \times \boldsymbol{k}\psi|^2 \rangle \tag{3.4}$$

associated with the function ψ stays relatively small in comparison to the kinetic energy of the poloidal component of motion as is evident from a comparison of

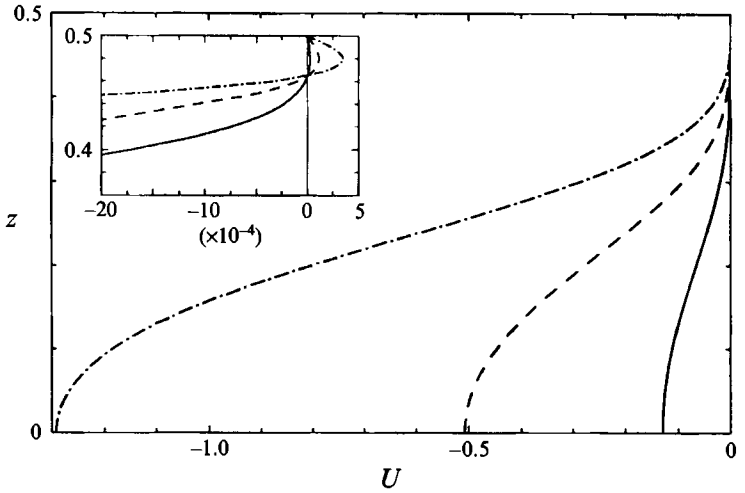

FIGURE 6. Profiles of the mean flow connected with blob convection travelling in the negative x-direction with $P = 7, \alpha_x = \alpha_y = 2.0$ and with $R = 28 \times 10^3$ (solid), $R = 35 \times 10^3$ (dashed), $R = 50 \times 10^3$ (dash-dotted). Because of the symmetry with respect to $z = 0$ only the upper part of the profile is shown. The insert shows the dependence near the boundary, $z = 0.5$, with an enlarged scale.

the values shown in figures 8 and 9. The kinetic energy of the mean flow shown in figure 10 increases approximately in proportion to $(R-R_{II})^2$ where R_{II} is the Rayleigh number for the onset of the respective blob oscillation. This dependence must be expected since the mean flow is generated by the product of velocity components with a sinusoidal dependence on x which grow with $(R-R_{II})^{1/2}$. The increase of the mean flow amplitude in proportion to $R-R_{II}$ shown in figure 6 also conforms to this expectation. The same dependence has been found in the mean flow generated by travelling waves in low Prandtl number convection (Clever & Busse, 1989). The frequency of oscillation of the travelling blobs is also displayed in figure 10. It increases in good approximation with R^n where n is a number slightly larger than $\frac{1}{2}$; in the case of figure 10 we find $n = 0.54$. This is nearly the same dependence with which the basic roll velocity increases as can be seen from figure 8 where the kinetic energy of the roll component increases more strongly than in proportion to R. This property emphasizes the fact that the blobs are carried around with the circulation of convection rolls.

4. Standing oscillatory blob convection

For the numerical study of standing oscillatory blob convection the forward integration in time of the basic equations (2.2) becomes necessary after the representation (2.4) with $c = 0$ has been introduced. Because of the much higher numerical effort the number of solutions that has been obtained is lower than in the case of travelling blob convection. Some reduction of the numerical effort can be obtained because all coefficients $\check{a}_{lmn}, \check{b}_{lmn}, \check{c}_{lmn}$ can be dropped from the representation (2.4) because without losing generality the symmetry plane $x = 0$ can be assumed.

As in other cases of standing oscillations, standing blob convection can be regarded as the superposition of two waves travelling in opposite directions. An impression of the standing oscillations can be gained from the variations in time of the vertical

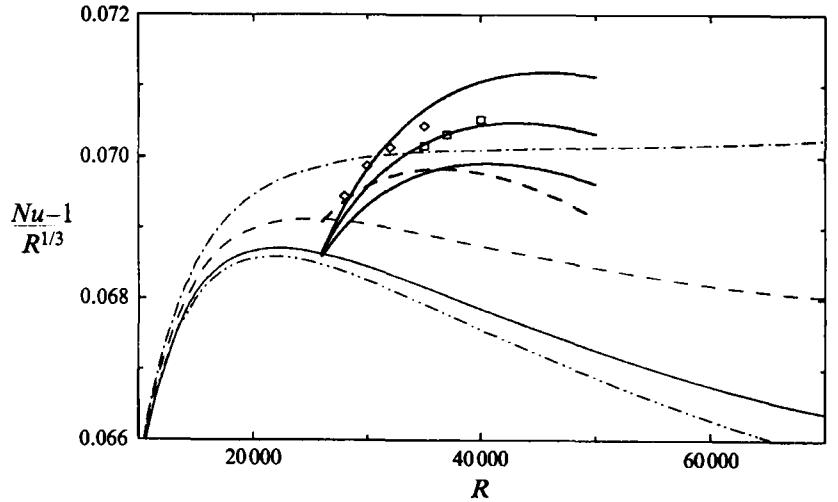

FIGURE 7. Nusselt number as a function of R, given by $Nu(R) - 1$, for two-dimensional convection rolls (thin lines) and for travelling blob convection (bifurcating thick lines). The cases $P = 2.5$ (dash-dotted line), $P = 4$ (dashed lines), $P = 7$ (solid lines) and $P = 10$ (dash-doubledotted line) are shown with $\alpha_y = 2.0$ in all cases. For the travelling blob convection the three thick solid curves correspond to $\alpha_x = 2.5, 2.0, 1.5$ (from top to bottom). The thick dashed curve corresponds to $\alpha_x = 2.0$. Also shown are the Nusselt numbers for standing blob convection in the cases $\alpha_x = 2.5$ ($\diamond$) and $\alpha_x = 2.0$ ($\square$) with $P = 7, \alpha_y = 2.0$ in both cases.

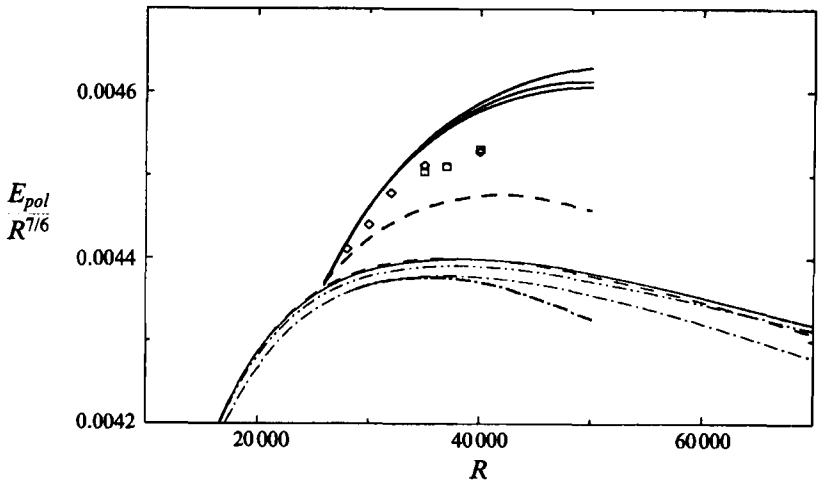

FIGURE 8. Kinetic energy of the poloidal component of motion, E_{pol}, as a function of R for two-dimensional rolls and for travelling blob convection for the same cases as in figure 7. As in figure 7 the symbols $\diamond$ and $\square$ refer to cases of standing blob convection.

velocity on three horizontal planes in the convection layer shown in figure 11. Only one half of the period of the oscillation is covered by the plots since the pattern is repeated in the second half of the period except for a shift by π/α_x along the axis of the original rolls. The variations of the isotherms in the plane $x = 0$ are shown in figure 12 for a full period of oscillation. The time dependence of the isotherms is similar to that exhibited by the travelling blob convection shown in figure 2 at a given plane $x = \text{const.}$, but it is less pronounced because of the lower Rayleigh number

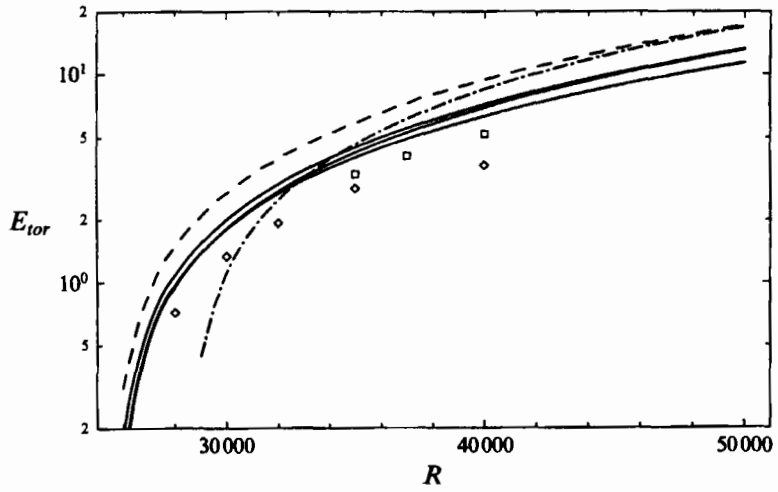

FIGURE 9. Kinetic energy of the toroidal component of motion, E_{tor}, for the same cases as in figures 7 and 8. In the case of the solid lines the uppermost, middle, and lowermost ones refer to $\alpha_x = 2.0, \alpha_x = 1.5$ and $\alpha_x = 2.5$, respectively.

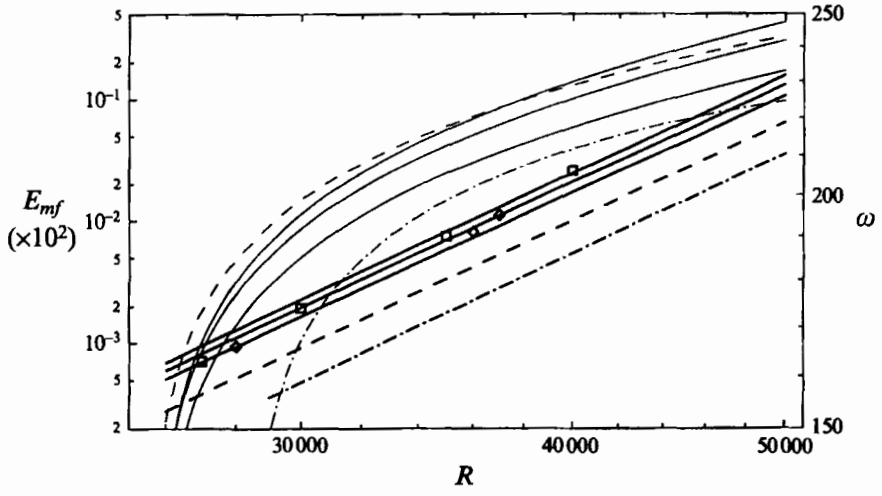

FIGURE 10. Kinetic energy of the mean flow component, E_{mf}, (thin lines, left ordinate) and the frequency ω of oscillations (thick lines, right ordinate) for the same cases of travelling blob convection as in figures 7 and 8. In the case of the solid lines E_{mf} increases and ω decreases with increasing α_x.

chosen in figure 12. The time dependence of the isotherms in the plane $x = \pi/\alpha_x$ is the same except that it is shifted in phase by half a period. On the other hand the isotherms in the plane $x = \pi/2\alpha_x$ show very little time dependence because this plane nearly represents the surface on which the standing oscillation vanishes. The plots of the x-velocity in the plane $x = \pi/2\alpha_x$ shown in figure 13 are rather similar to the corresponding plots for travelling blob convection shown in figure 5. Because of the symmetry

$$v_x(x, y, z, t) = -v_x(-x + \pi/2\alpha_x, y, z, t + T_p/2) \tag{4.1}$$

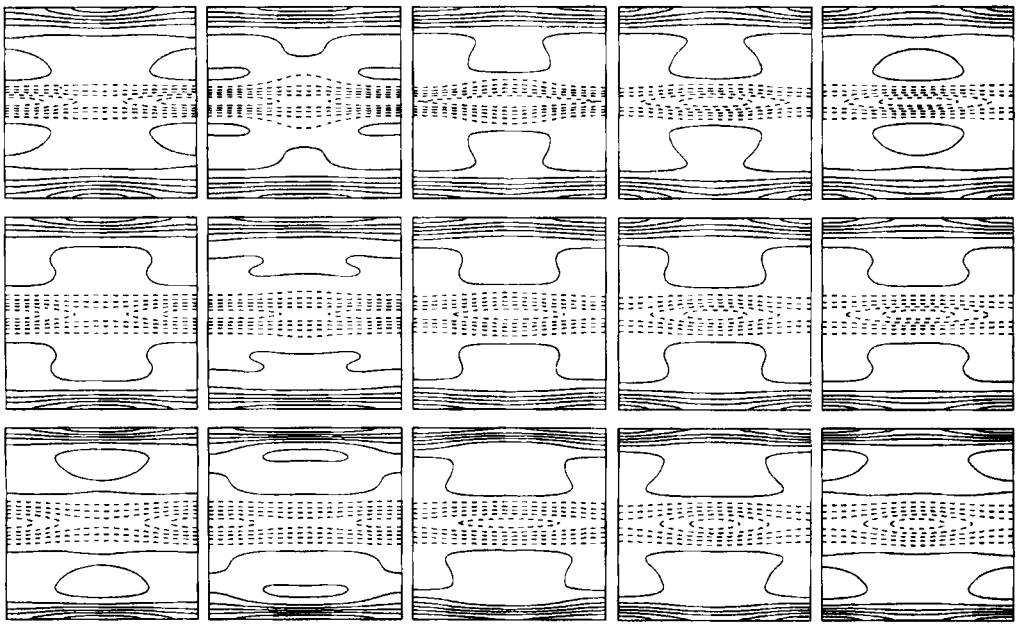

FIGURE 11. Lines of constant vertical velocity for standing blob convection in the planes $z = -0.4$ (upper row), $z = 0$ (middle row), and $z = -0.4$ (lower row) for 5 equidistant times such that a half-period, $0.5T_p = 0.0192$, of oscillation is covered in each row. Parameters are $P = 7, R = 27000, \alpha_x = \alpha_y = 2.0$.

where T_p is the period of oscillation, standing blob convection does not give rise to a mean flow in the x-direction. The oscillations of the x-velocity reach a maximum in the planes $x = (n + \frac{1}{2})\pi/\alpha_x$, but vanish in the planes $x = n\pi/\alpha_x$ for all integer values n.

The close similarity between standing and travelling oscillations is also evident from the Nusselt numbers and kinetic energies shown in figures 7–10. The standing blob solutions do not exhibit a mean flow component and for this reason the energy of the toroidal component of motion is also lower than in the case of the travelling blob solution. This property is a result of the fact that part of the toroidal component is generated through the advection of the mean flow by the basic rolls.

5. Instabilities of oscillatory blob convection

The transition from two-dimensional roll convection to oscillatory blob convection in its two manifestations represents a typical Hopf bifurcation in the presence of symmetry. Because a Hopf bifurcation is characterized by the property that an eigenvalue and its complex conjugate cross the imaginary axis simultaneously, there must be two time-dependent solutions. The translation invariance along the axis of the rolls and the reflection symmetry with respect to any plane $x = \text{const.}$ are the symmetries governing the Hopf bifurcation. Accordingly the bifurcating time-periodic solutions assume either the form of a travelling wave or of a standing wave (Schecter 1976; Golubitsky & Stewart 1985). In the latter paper it has also been demonstrated that just one of the two solutions is stable in the case when both bifurcations are supercritical. In terms of the coupled amplitude equations discussed in the mathematical context, it is found that the solution with the larger amplitude

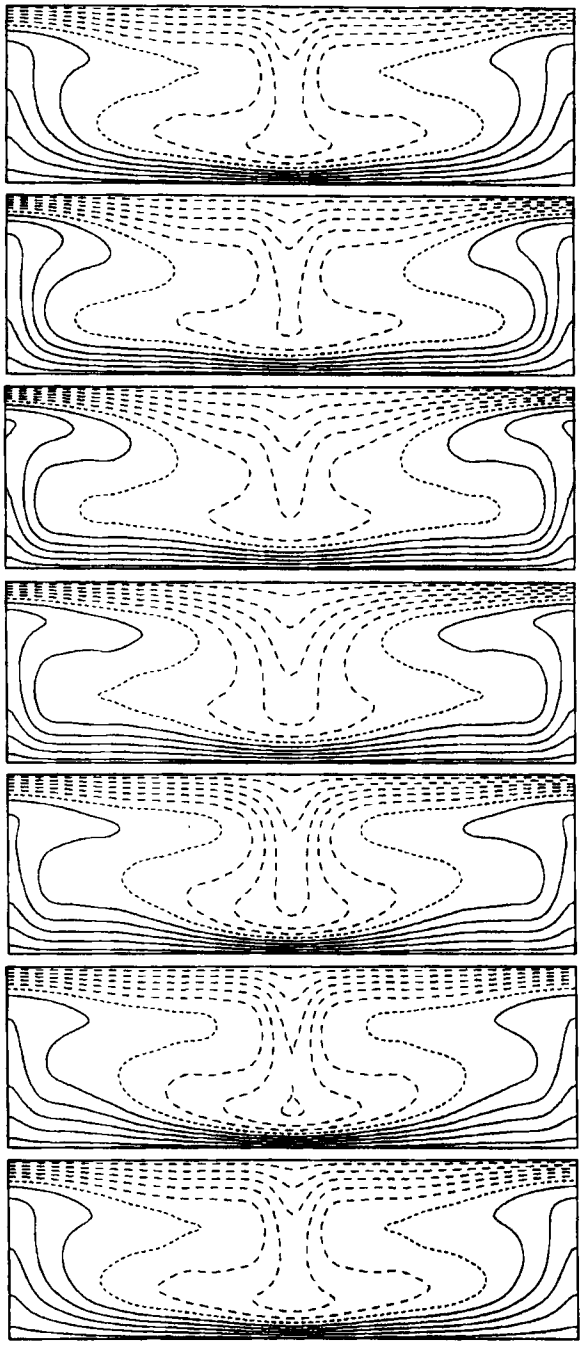

FIGURE 12. Isotherms in the plane $x = 0$ for standing blob convection with $P = 7, R = 28000, \alpha_x = 2.5, \alpha_y = 2.0$ at equally distant times $t_n = n \times 0.0063$ with $n = 0, \ldots, 6$ (from top to bottom) such that about one period, $T_p = 0.0378$, is covered by the plots.

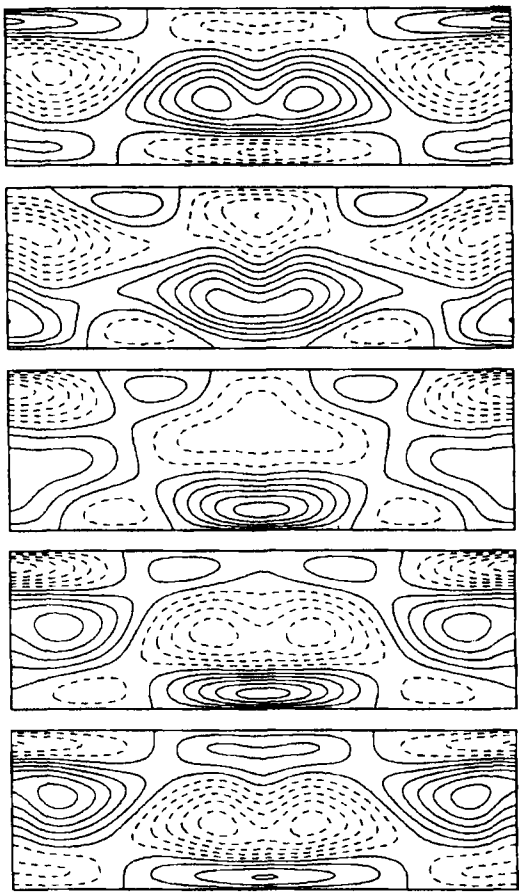

FIGURE 13. Lines of constant x-velocity, v_x, in the plane $x = \pi/2\alpha_x$ for standing blob convection with $P = 2.5, R = 30000, \alpha_x = 2.5, \alpha_y = 2.0$ at equally distant times $t_n = n \times 0.005$ with $n = 0, \ldots, 4$ such that about one half of the period $T_p \approx 0.040$ is covered by the plots.

is preferred. As we shall discuss in the following, the stability analysis of the blob solutions confirms this expectation.

The stability analysis of travelling blob convection is fairly straightforward once the class of disturbances of the form (2.6) is reduced to those with the Floquet wavenumbers $b = d = 0$. Since the blob solutions are characterized by fields φ, θ that are symmetric in y, the disturbance fields $\tilde{\varphi}, \tilde{\theta}$ with $b = d = 0$ separate into those that are symmetric (C) or antisymmetric (S) in the y-direction. The y-symmetry of the fields $\psi, \tilde{\psi}$ is, of course, always opposite to that of $\varphi, \tilde{\varphi}$, respectively. The disturbances also separate into those with vanishing coefficients for $l + m + n =$ odd (E) and those with vanishing coefficients for $l + m + n =$ even (O). We thus have to consider four different classes

$$EC,\ ES,\ OC,\ OS$$

of disturbances. Among these the first class, EC, exhibits the same symmetries as the travelling blob solution. The results of the stability calculations are given in table 1 in terms of the critical Rayleigh number R_{III} at which the real part of the growth rate goes through zero. In some cases when the growth rate exhibits a particular strongly varying real part the second lowest Rayleigh number for the onset

P	α_x	α_y	Nu at $R = 4 \times 10^4$ for $N_T = 14(12)$	Symmetry of critical dist.	$R_{III} \times 10^{-4}$	σ_i	$\frac{\partial \sigma_r}{\partial R} \times 10^3$
2.5	2.0	2.0		*OC*	3.23	224	1.5
4	2.0	2.0	3.3949 (3.4079)	*OS*	3.70	247	1.4
7	1.5	2.0	3.3980 (3.4089)	*EC*	2.69	166	0.2
	2.0	2.0	3.4169 (3.4285)	*OC*	4.54	228	0.1
				OC	4.63	516	1.1
	2.5	2.0	3.4586 (3.4513)	*OC*	4.23	219	0.2
				OC	4.49	295	1.1

TABLE 1. Instabilities of travelling blob convection

of a disturbance has also been indicated since it may be observed as the preferred instability in experiments. $N_T = 14$ has been used for the travelling blob solution as well as for the stability analysis. The comparison of the Nusselt numbers for $N_T = 12$ and $N_T = 14$ at the fairly high Rayleigh number $R = 4 \times 10^4$ provides a measure for the quality of the approximation.

We can also investigate the stability of the standing blob convection by superimposing disturbances with the same horizontal periodicity interval , but with x- and y-symmetries differing from those of standing blob convection and by following their temporal evolution with the help of a forward integration in time through a full period of oscillation. In this way it has been found that the standing oscillations are always unstable with respect to travelling blob convection. This result is in qualitative agreement with the theory of Golubitsky and Stewart (1989), since the latter solution exhibits a somewhat higher amplitude than the former solutions, at least as far as the kinetic energy of motion is concerned, according to the results displayed in figures 8 and 9.

6. Discussion

In contrast to convection in a horizontal layer of a low Prandtl number fluid for which much observational evidence and considerable theoretical understanding for travelling wave convection has been achieved (for a review see Busse 1981), there do not seem to be any reported measurements of the properties of travelling blob convection in fluids with Prandtl numbers in excess of unity. In fact it has been surprising to the authors of this paper to recognize the preference for this type of propagating convection wave. The parameter range where travelling blob convection can be expected is not very large, of course, and other instabilities leading from two-dimensional rolls to three-dimensional convection are more commonly encountered in the relevant Prandtl number range. But in a water layer in which rolls of sufficiently large wavelength have been induced through the method of Chen & Whitehead (1968) it should be possible to realize travelling blob convection. For a water layer of 1 cm depth at room temperature a Rayleigh number of the order of 4×10^4 is reached for $T_2 - T_1 \approx 3\,^\circ\mathrm{C}$ and oscillations with a period of 20 s should be observable. The mean flow would have a magnitude of only 1 mm min^{-1} in this case, but would increase strongly with the Rayleigh number.

There is some evidence that a process akin to the mechanism of travelling blob convection becomes more prevalent at higher Rayleigh numbers. Travelling tilted plumes similar to those shown in figure 4 have been observed by Krishnamurti &

Howard (1981) in a water layer for Rayleigh numbers above 2×10^6. Because of this high Rayleigh number at which convection in a water layer is already quite turbulent, a direct comparison with the calculations of this paper is not possible. On the other hand, the mechanism of travelling tilted plumes and of mean flow generation discussed in §3 is quite different from the two-dimensional model proposed by Howard & Krishnamurti (1986) or the two-dimensional analysis of Prat, Massaguer & Mercader (1995). There is no evidence that there is a two-dimensional instability of convection rolls associated with a mean flow in a non-rotating convection layer at Rayleigh numbers below the onset of three-dimensional instabilities. The generation of mean flows by nearly two-dimensional convection rolls driven by centrifugal buoyancy in a rotating cylindrical annulus is a well-known phenomenon that has been explored experimentally and theoretically (Busse & Hood, 1982; Or & Busse 1987). But in non-rotating layers such a mechanism is always preceded by the transition to three-dimensional forms of convection. Of course, the two-dimensional model of Howard & Krishnamurti (1986) was not meant to predict the detailed spatial structure of the convection with mean flow and may be more directly applicable for convection in a Hele-Shaw cell for which independent observational evidence exists. It is also important to note in connection with the travelling blob mechanism that the fluctuating component of motion along the axis of the basic rolls is mainly antisymmetric in z and attains even higher amplitudes than the mean flow.

Oscillatory thermal blobs are most commonly observed when they are preceded by a transition to three-dimensional convection at a lower Rayleigh number. The transitions from steady to oscillatory knot convection or from steady to oscillatory bimodal convection are the best known examples (Clever & Busse 1988, 1994). Because of the absence of a translation-invariant dimension, travelling blob convection is prohibited in these cases. The oscillatory thermal blobs represent a very robust phenomenon, however, which is still evident in turbulent convection. Under certain circumstances it seems that even the travelling wave mechanism, together with the mean flow effect, can overcome the constraints imposed by the absence of the translation-invariant dimension in turbulent convection and give rise to the phenomenon observed by Krishnamurti & Howard (1981).

For future research it will be interesting to investigate the patterns of convection which replace travelling blob convection after the onset of the instabilities listed in table 1. Asymmetric traveling waves or vacillating waves of blob convection are likely to be introduced by these bifurcations. Mechanisms such as the mean flow generation mechanism tend to persist, however, and we thus expect mean flows to be associated with those more complex forms of convection.

The research reported in this paper has been supported under Grant ATM 92-09335 of the US National Science Foundation and by a NATO travel grant.

REFERENCES

BOLTON, E. W., BUSSE, F. H. & CLEVER, R. M. 1986 Oscillatory instabilities of convection rolls at intermediate Prandtl numbers. *J. Fluid Mech.* **164**, 469–485.

BUSSE, F. H. 1967 On the stability of two-dimensional convection in a layer heated from below. *J. Math. Phys.* **46**, 140–150.

BUSSE, F. H. 1981 Transition to turbulence in Rayleigh-Bénard convection. In *Hydrodynamic Instabilities and the Transition to Turbulence* (ed. H. L. Swinney & J. P. Gollub). Springer.

BUSSE, F. H. & CLEVER, R. M. 1979 Instabilities of convection rolls in a fluid of moderate Prandtl number. *J. Fluid Mech.* **91**, 319–335.

BUSSE, F. H. & CLEVER, R. M. 1990 Transitions to more complex patterns in thermal convection. In *New Trends in Nonlinear Dynamics and Pattern Forming Phenomena: The Geometry of Nonequilibrium* (ed. P. Coullet & P. Huerre), pp. 37–45. NATO ASI Series, Plenum.

BUSSE, F. H. & HOOD, L. L. 1982 Differential rotation driven by convection in a rotating annulus. *Geophys. Astrophys. Fluid Dyn.* **21**, 59–74.

BUSSE, F. H., KROPP, M. & ZAKS, M. 1992 Spatio-temporal structures in phase-turbulent convection. *Physica* D **61**, 94–105.

CHEN, M. M. & WHITEHEAD, J. A. 1968 Evolution of two-dimensional periodic Rayleigh convection cells of arbitrary wavenumbers. *J. Fluid Mech.* **31**, 1–15.

CLEVER, R. M. & BUSSE, F. H. 1987 Nonlinear oscillatory convection. *J. Fluid Mech.* **176**, 403–417.

CLEVER, R. M. & BUSSE, F. H. 1988 Three-dimensional knot convection in a layer heated from below. *J. Fluid Mech.* **198**, 345–363.

CLEVER, R. M. & BUSSE, F. H. 1989 Nonlinear oscillatory convection in the presence of a vertical magnetic field. *J. Fluid Mech.* **201**, 507–523.

CLEVER, R. M. & BUSSE, F. H. 1990 Convection at very low Prandtl numbers. *Phys. Fluids* A **2**, 334–339.

CLEVER, R. M. & BUSSE, F. H. 1993 Convection in a fluid layer with asymmetric boundary conditions. *Phys. Fluids* A **5**, 99–107.

CLEVER, R. M. & BUSSE, F. H. 1994 Steady and oscillatory bimodal convection. *J. Fluid Mech.* **271**, 103–118.

CURRY, T. B., HERRING, J. R., LONCARIC, J. & ORSZAG, S. A. 1984 Order and disorder in two- and three-dimensional Bénard convection. *J. Fluid Mech.* **147**, 1–38.

FRICK, H., BUSSE, F. H. & CLEVER, R. M. 1983 Steady three-dimensional convection at high Prandtl number. *J. Fluid Mech.* **127**, 141–153.

GOLLUB, J. P., MCCARRIAR, A. R. & STEINMAN, I. F. 1982 Convective pattern evolution and secondary instabilities. *J. Fluid Mech.* **125**, 259–281.

GOLUBITSKY, M. & STEWART, I. 1989 Hopf bifurcation in the presence of symmetry. *Arch. Rat. Mech. Anal.* **87**, 107–165.

HOWARD, L. N. 1966 Convection at high Rayleigh number. In *Proc. 11th Intl Congr. Appl. Mech., Munich 1964* (ed. H. Görtler), pp. 1109–1115. Springer.

HOWARD, L. N. & KRISHNAMURTI, R. 1986 Large-scale flow in turbulent convection: a mathematical model. *J. Fluid Mech.* **170**, 385–410.

KRISHNAMURTI, R. & HOWARD, L. N. 1981 Large-scale flow generation in turbulent convection. *Proc. Natl Acad. Sci. USA* **78**, 1981–1985.

LENNIE, T. B., MCKENZIE, D. P., MOORE, D. R. & WEISS, N. O. 1988 The breakdown of steady convection. *J. Fluid Mech.* **188**, 47–85.

OR, A. C. & BUSSE, F. H. 1987 Convection in a rotating cylindrical annulus. Part 2. Transitions to asymmetric and vacillating flows. *J. Fluid Mech.* **174**, 313–326.

PRAT, J., MASSAGUER, J. M. & MERCADER, I. 1995 Large-scale flows and resonances in 2-D thermal convection. *Phys. Fluids* **7**, 121–134.

SCHECTER, S. 1976 Bifurcations with symmetry. In *The Hopf Bifurcation and its Applications* (ed. J. E. Marsden & M. McCracken), pp. 224–249. Springer.

SCHMITT, B. J. & WAHL, W. VON 1992 Decomposition of solenoidal fields into poloidal fields, toroidal fields and the mean flow. Applications to the Boussinesq-equations. In *The Navier-Stokes Equations II - Theory and Numerical Methods* (ed. J. G. Heywood, K. Masuda, R. Rautmann, S. A. Solonnikov). Lecture Notes in Mathematics, vol. 1530, pp. 291–305. Springer.

SOLOMON, T. H. & GOLLUB, J. P. 1990 Sheared boundary layers in turbulent Rayleigh-Bénard Convection. *Phys. Rev. Lett.* **64**, 2382–2385.

ZIPPELIUS, A. & SIGGIA, E. D. 1983 Stability of finite amplitude convection. *Phys. Fluids* **26**, 2905–2915.

ZOCCHI, G., MOSES, E. & LIBCHABER, A. 1990 Coherent structures in turbulent convection, an experimental study. *Physica* A **166**, 387–407.